

M 10 | R.J.Davis et al.: Palladseite

PALLADSEITE, A NEW MINERAL FROM ITABIRA, MINAS GERAIS, BRAZIL

R.J. Davis, A.M. Clark, and A.J. Criddle

Department of Mineralogy, British Museum
(Natural History), Cromwell Road, London SW7 5BD

Clark *et al.* (1974) reported on the first part of an examination of the residual concentrates from the gold workings at Itabira, Minas Gerais, Brazil, contained in specimen number BM 1934.72. The concentrates were presented to the Mineralogy Department of the British Museum (Natural History) by Bernard Hall Sanders. The mainly monomineralic grains (apart from surface deposits) consist dominantly of arsenopalladinite, with rarer atsenite and isometeite, all three being new minerals, essentially arsenide-antimonides of palladium. In a survey under the electron microprobe of grains selected at random from BM 1934.72 Clark *et al.* found Grain 1 containing major palladium and selenium and minor copper. In a parallel survey by X-ray single crystal methods of randomly selected grains we found Grain 2, identified from its cubic cell dimensions as a palladium selenide near PdSe in composition. Grains 1 and 2 proved to be identical, and further grains were later discovered by optical and microprobe methods. The latter form the type specimens of a new mineral, palladseite, named from the chemical composition (PALLADIUM SELENIde), and approved by the Commission on New Minerals and Mineral names, International Mineralogical Association.

Palladium selenide minerals are very rare. Besides major palladium and selenium, oosterboschite, (Pd,Cu)₁₇Se₁₅ (Johan *et al.*, 1970) contains 17% copper, which is probably essential. Zincken (1829) found selenopalladium in clausthalite ores from Tilkeroede, Harz, but he later withdrew verbally the presence of selenium. There is an extensive literature on synthetic palladium selenides (see Bibliography), which shows that palladium selenides near PdSe in composition are present in the anode sludges from the electrolytic purification of copper (Ignatov and Flaksin, 1958; Dolivo-Debrovo'skii, 1964; Graefver, 1965), and in residual sludges after the purification of silver (Blicksilver) from silver coins (Rösel, 1876).

Specimen preparation. Five grains were prepared for reflected light microscopy and electron probe microanalysis. They were mounted in a cold setting epoxy resin and, owing to their size (0.2 - 0.5 mm), polished without pre-grinding on Hypocel-pellon laps with diamond abrasives 6µm, 3µm and 1µm. Polishing was completed with 1/4 µm diamond paste on cloth laps. Ethanol and distilled water were used together as the lubricant at all the polishing stages.

Optical characteristics: Palladseite is isotropic. In plane polarized light it is white except when compared with the other minerals of the Itabira concentrates, atsenite, arsenopalladinite and isometeite, (see Clark *et al.* 1974) where it appears grey and lacking any detectable spectral hue. The grains have smooth (straight and curvilinear) margins; they are subangular, anhedral to subhedral. The largest grains, 1 and 5, are monomineralic while grains 2-4 contain inclusions. Grain 3 contains inclusions of the two lower reflecting minerals found separately in grains 2 and 4. Both inclusion phases are isotropic; they occur intergrown together as discrete grains 1-4µm in size with round cornered, square outlines; the lower reflecting grey phase encloses rectangular cores of the higher reflecting phase. They also occur as aggregated clusters of smaller rounded grains (grain size < 1µm - 2µm, aggregated up to 5µm) and as subangular wedges, or fingers, penetrating the palladseite grain from its rim, with a maximum length of 6µm and width of 4µm. The small size of these

TABLE I. Electron probe analyses and cell dimensions of three palladseite grains. A = Weight per cent, B = atomic proportions based on 32 atoms per formula unit.

	Grain 1		Grain 2		Grain 3	
	A	B	A	B	A	B
Pd	55.77	15.47	55.13	15.17	55.47	15.38
Pt	0.00	0.00	0.39	0.06	0.04	0.01
Cu	3.99	1.85	4.33	1.99	3.89	1.80
Hg	1.66	0.26	1.24	0.18	1.68	0.25
Se	38.99	14.43	39.38	14.60	38.97	14.56
	100.01		100.47		100.05	
$\frac{A}{B}$	10.635(2)		10.628(4)		10.640(2)	

inclusions precluded the use of quantitative reflectance and chemical analyses, but qualitative probe scans indicate that both phases are copper-bearing oxides of palladium. As they are isotropic they are unlikely to be palladinite, the only oxide of palladium previously reported.

Chemical composition. Electron probe analyses of grains 1, 2 and 3, given in Table I, were obtained by measuring Pd, Pt, and Cu relative to pure metal standards, Hg against cinnabar, and Se against synthetic clausthalite, PdSe. The instrument used was a Cambridge Geoscan and the measurements were made at an accelerating potential of 20 keV. The measured intensities, after dead time corrections, were processed with the BM-IC-NPL computer programme (Mason *et al.*, 1969) to give the tabulated weight percentages. Recalculation of these analyses to a total of 32 atoms approached the ideal formula (Pd, Cu)₁₇Se₁₅ in each case. The three analyses are virtually identical apart from the presence of minor Pt in Grain 1. The selenium concentration is similar to that given for oosterboschite (Johan *et al.*, 1970) and until the X-ray and optical data proved otherwise, palladseite was thought to be a Cu-poor oosterboschite.

Table II. Reflectivity data

nm	GRAIN 1		GRAIN 2		GRAIN 3		GRAIN 4
	air	oil	air	oil	air	air	
400	40.3	26.0	39.9	27.4	41.0	42.1	
420	41.2	26.9	40.9	28.3	41.6	42.6	
440	42.2	27.7	41.8	28.9	42.3	43.1	
460	42.8	28.6	42.5	29.5	42.8	43.6	
470	43.1	28.9	43.0	29.8	43.1	43.8	
480	43.4	29.1	43.0	30.0	43.4	44.0	
500	44.0	29.5	43.4	30.4	43.8	44.4	
520	44.4	29.9	44.0	30.6	44.3	44.8	
540	44.8	30.1	44.5	30.9	44.6	45.2	
560	44.9	30.1	44.5	31.0	44.7	45.2	
580	45.0	30.2	44.6	31.0	44.8	45.3	
590	45.1	30.2	44.8	31.0	44.9	45.3	
600	45.1	30.1	44.8	30.9	44.9	45.2	
620	45.0	30.0	45.1	30.8	44.8	45.1	
640	45.1	30.1	45.6	30.9	44.9	45.1	
660	45.0	30.1	45.5	31.0	44.9	45.2	
680	45.1	30.0	45.6	31.0	45.1	45.2	
700	45.2	30.5	46.0	31.8	45.4	45.8	

Table III. Quantitative colour values

Illuminant C						
x	0.3144	0.3148	0.3150	0.3143	0.3143	0.3131
y	0.3226	0.3243	0.3221	0.3229	0.3219	0.3211
z	0.3629	0.3609	0.3628	0.3630	0.3638	0.3658
λ_D	572.5	570.4	575.3	570.9	573.8	571.5
P% _g	2.87	3.41	2.89	2.84	2.64	2.09
Y	44.72	29.98	44.44	30.79	44.59	45.03
Illuminant A						
x	0.4504	0.4503	0.4514	0.4500	0.4506	0.4494
y	0.4403	0.4411	0.4406	0.4405	0.4408	0.4408
z	0.1393	0.1385	0.1390	0.1395	0.1396	0.1409
λ_D	581.3	579.5	584.4	579.9	582.5	579.7
P% _g	3.89	4.42	4.08	3.74	3.68	2.81
Y	44.83	30.04	44.61	30.84	44.71	45.09

The values in Table III are relative to the CIE(1931) illuminants C and A which have colour temperatures of 6770°K and 2854°K respectively. The rectangular chromaticity co-ordinates, x, y and z, and the Helmholtz values, Y the luminance, λ_D the dominant wavelength and P% the excitation purity, were computed using the weighted ordinate method.

$$N = h^2 + k^2 + l^2$$

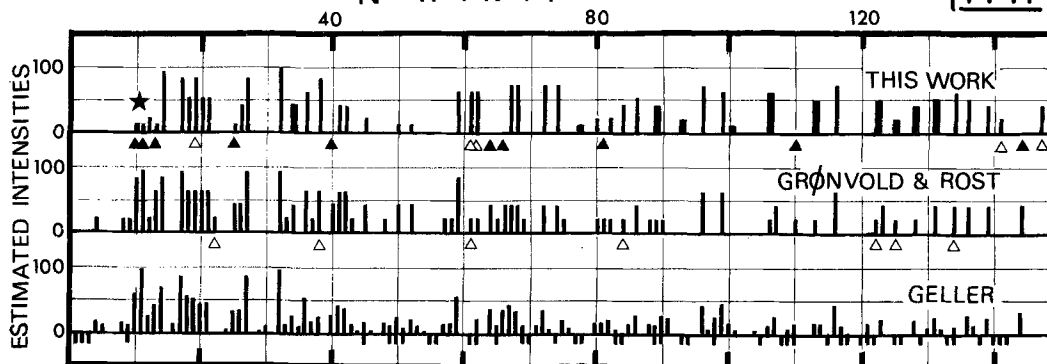


Fig.1. X-ray powder patterns for palladseite. For explanation see text.

Quantitative microscopy: R values in air and Cargille A oil for grain 1 were obtained from 420-700 nm at intervals of approximately 10 nm using the equipment described in Clark *et al.* (1974). Grains 2 to 4 were measured with a Zeiss Universal microscope equipped with photometer MPMO3, photomultiplier R446 and a continuous line interference filter. Measurements were made in air for all the grains and with Zeiss oil for grain 2, from 400-700 nm at 20 nm intervals. A Zeiss WTiC standard (no. 266) was used with a pair of X16 air and oil objectives.

The spectral reflectance values in air for the different grains, Table II, are relatively constant and, over the visible spectrum range, at least, are not obviously sensitive to minor chemical variation. The R values for the two grains measured in oil differ in magnitude at different wavelengths by up to 1.4% relative, but the shape of the curve are similar. Quantitative colour values were computed with an unpublished programme developed by G.S. Bearne, M. Hills and Miss K. Shaw for use with an HP 9830 programmable calculator. The programme used Wright's (1964, Table 8, p.276) condensed tables for the CIE (1931) system of distribution coefficients weighted by energy values for the illuminants S_A and S_C . The reflectances used in the calculations are those shown in Table II (excluding the COM wavelengths) and R values which were interpolated from these at intervals of 10nm. The quantitative colour values so derived for the four grains are similar, Table III. The excitation purity levels are low and the luminance is quite high for both illuminants which explains why the mineral lacks any detectable hue in reflected light (observations were made using a quartz halogen light source, the colour temperature of which approximates to that of illuminant A). It will be seen that the excitation purity and the luminance levels for the A source are higher than for the C source, and that the dominant wavelengths are shifted by about 9nm towards the orange. This is to be expected since the A source is 'cooler', with a lower emission in the blue part of the spectrum than the C source.

The grey appearance of palladseite against the other Itabira species is a result of its lower excitation purity and luminance levels; the dominant wavelengths for the four species (C source) being between 565 and 583nm (Table VII, p547, Clark *et al.* 1974). The isotropy, luminance level, and shape of the reflectance curves readily distinguish palladseite from the anisotropic lamellar twinned oosterboschite (Johan *et al.* 1970), and from all the previously reported platinum group minerals. Carrolite, $Cu(Co,Ni)_2S_4$. (Bovis *et al.* 1975) is the only mineral previously reported with similar reflectance properties. However, at the four C.O.M. wavelengths, the reflectance values of carrolite are consistently 7% lower than those of palladseite and the VHN_{100} of palladseite (measured by G.S. Bearne) is 474 (350-437) compared with 351-366 for carrolite.

X-ray studies. Grain 2 from the X-ray survey proved to be cubic whereas oosterboschite is orthorhombic (Johan *et al.*, 1970). A rotation photograph around [011] showed sharp spots on 15 Å layer lines plus smooth powder lines due to microcrystalline potarite. Laue photographs taken along [100] [111], and [011] showed 4mm, 2m, and 2mm symmetries respectively. Back-reflection oscillation photographs with the mean beam position along [100] and [011] respectively gave accurate cell dimensions (Table IV) with a value of $(a/b)_{(011)}^2 = 1.9996(8)$. Weissenberg photographs showed no systematic absences, so that the space group is one of $Fm\bar{3}m$, $Fd\bar{3}m$ or $Fm\bar{3}2$. Using an

approximate cell dimension of 10.6Å the tables of Donnay and Ondik (1975) identified grain 2 as a palladium selenide near PdSe and variously formulated as $Pd_{1.1}Se$, Pd_9Se_8 , or, correctly, as $Pd_{17}Se_{15}$ of Geller (1962). This identification was confirmed when Grain 1, already analysed, gave a rotation photograph around [100] identical (apart from the potarite lines) with a similar photograph of Grain 2.

The original Gandolfi "powder" photograph was supplemented by two further such photographs after re-mounting Grain 1, and by one each from Grains 3 and 4 mounted at random. Accurate cell dimensions derived by extrapolation methods are listed in Table IV, and are discussed below.

Fig. 1 shows a typical Gandolfi pattern of Grain 1, the pattern of $Pd_{17}Se_{15}$ (Gronvold and Rost, 1956; also PDF Card 11-508), and the pattern calculated from those structure factors, F_{obs}^* , measured by Geller (1962).

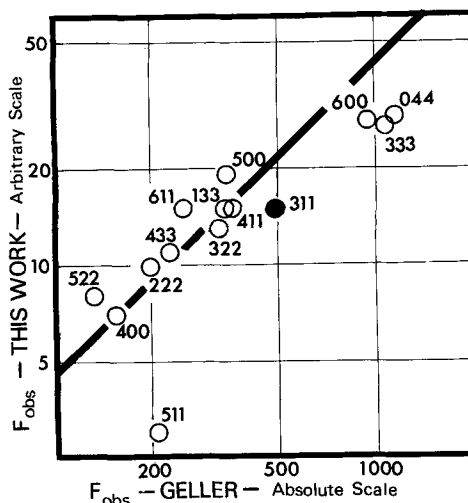


Fig.2. Structure factors for palladseite measured here, and plotted against the values given by Geller (1962).

1. Visually estimated line intensities on the two observed patterns are plotted on the usual scale from $\sqrt{100}$ to $\sqrt{10}$, which correlates better with the square root rather than the first power of the calculated intensity. Accordingly for Geller's data we plot values of $O.O_{100} \times (\sum p_i^2 F_{obs}^*)^{1/2}$ where p_i is the reflection multiplicity and d_i^2 is the interplanar spacing; d_i^2 measures most of the angular variation in the Lorentz polarization factor.

M 12 I

Table IV. Cell dimensions for palladseite and $\text{Pd}_{17}\text{Se}_{15}$. Unless otherwise stated all results were obtained with filtered Cu-K α radiation, using 6 cm diameter back reflection cameras for single crystal rotation (R) and oscillation (O) photographs and cameras of 11.46 cm diameter for powder (P) and Gandolfi (G) photographs

Palladseite				$\text{Pd}_{17}\text{Se}_{15}$		
Grain	a Å	Notes	Authors	a Å	Notes	
1	10.635 ₆ (1)	O	Gronvold and Rost (1956)	10.604	P	
1	10.636 ₆ (1)	O	Schubert et al. (1957)	10.64	†	
1	10.633 ₃ (1 ₂)	R	Kjekshus (1960)	10.6060(1)	P	
2	10.628(4)	G	Geller (1962)	10.606(5)	P	
3	10.640(5)	R				
3	10.640(4)	G				
3	10.640(2 ₂)	G*				
4	10.631(4)	G				

* Filtered Co-K α radiation used.

† No experimental details given. Result converted from 10.62 kX using factor 1.002023.

Figures in brackets are estimated errors in the last unbracketed digit. Grains 2 and 3 were pure; 3 and 4 contained PdO.

Thermal expansion coefficient of $\text{Pd}_{17}\text{Se}_{15}$ is $9.8 \times 10^{-6}/^{\circ}\text{C}$, equivalent to 0.000104 Å/ $^{\circ}\text{C}$ in the cell dimensions (Kjekshus, 1960)

Lines below Geller's pattern suggest that his unmeasured structure factors and triangles indicate significant discrepancies between our pattern and that of $\text{Pd}_{17}\text{Se}_{15}$ or between the latter and Geller's data. Some lines graded as vvw in Geller's pattern are undetected by Gronvold and Rost, but of their seven anomalously strong lines (empty triangles) five can be attributed to Geller's unmeasured structure factors and in general the agreement is excellent. However, our pattern shows ten anomalously weak lines (full triangles) as well as five anomalously strong ones (empty triangles). This is mainly attributed to the known imperfections (see e.g. Gabri et al., 1975) in Gandolfi patterns and we were only disturbed by the lines at N=10, 11, and 13, which we graded as vvw but were given as g, vs, and m respectively by Gronvold and Rost. Since the 311 line at N = 11 is taken as the strongest on PDF Card 11-508, our earlier failure to identify palladseite is explained. We therefore took the additional Gandolfi photographs of grains mounted at random but only on one of these did the intensities of these lines rise above m, whereas the line at N = 14, graded as g by Gronvold and Rost, always lay in the range mg to vs in our patterns.

Fig. 2 shows structure factors obtained in the usual way from visual estimates of the blackening of all spots on our hkl Weissberg photograph out to N=36, plotted with a line of unit slope on a log-log scale versus the corresponding structure factors of Geller. We have evidently underestimated the blackening of three very strong spots and one very weak one but there is, in general, good agreement between our values and those of Geller, showing that palladseite is isostructural as well as isomorphous with $\text{Pd}_{17}\text{Se}_{15}$ and particularly that the intensity of the 311 spot agrees with Geller's value. Discrepancies in fig. 1 are therefore artefacts and we offer in Table V powder data for palladseite, taken from Gronvold and Rost (1956). The intensity differences are not thought to be caused by copper substituting for some of the palladium in palladseite.

Synthetic palladium selenides. Palladium selenide precipitated from a solution of a palladous salt analyses at stoichiometric PdSe, but has not been examined by X-ray diffraction. Bessler (1896) and Tsimmi and Rakshpal (1961) found the precipitate reasonably stable but Noser and Atynski (1925) note that it cannot be heated or dried without decomposition. Gronvold and Rost (1956) heated an alloy of composition PdSe in an evacuated silica capsule at 500-800°C and found that it then gave a dominantly cubic X-ray powder pattern close to that of "Rh₃S₈"¹ together

1. This compound was later shown to be Rh₁₇S₁₅, isostructural with palladseite

with the strongest lines of PdSe₂. After adding sufficient palladium to bring the composition to Pd₁₇Se₁₅, the alloy was reheated at 600°C when it gave the powder pattern of the pure cubic phase with a density of 8.30 g.cm⁻³ and a = 10.60 Å. For an assumed formula of Pd₁₇Se₁₅ unit cell contents are

TABLE V. X-ray powder data for palladseite

N	d	I _P	I _G	N	d	I _P	I _G
4	5.29	v	a	61	1.356	v	m
8	3.73	v	a	62	1.346	v	m
9	3.51	v	a	64	1.324	w	a
10	3.34	s	v	65	1.315	v	a
11	3.18	vs	v	66	1.304	w	a
12	3.06	v	v	67	1.295	w	ms
13	2.932	m	v	68	1.284	w	ms
14	2.827	s	vs	69	1.275	v	a
17	2.563	vs	s	72	1.248	w	ms
18	2.491	m	w	74	1.222	w	ms
19	2.426	m	s	75	1.224	v	a
20	2.365	m	mw	77	1.208	a	v
21	2.037	m	mw	80	1.185	v	v
22	2.261	v	a	81	1.178	v	a
25	2.118	w	v	82	1.171	v	v
26	2.074	w	w	84	1.157	v	w
27	2.037	vs	s	86	1.143	w	m
32	1.870	vs	v	88	1.130	v	w
33	1.842	v	a	89	1.123	v	w
34	1.814	w	w	90	1.117	v	a
36	1.764	m	m	93	1.099	a	v
37	1.739	v	v	96	1.081	m	ms
38	1.715	m	s	99	1.065	m	m
40	1.675	w	a	100	1.060	a	v
41	1.653	m	w	106	1.029	v	w
42	1.634	m	w	107	1.024	w	a
43	1.614	v	a	110	1.010	v	a
45	1.578	w	v	113	0.997	v	w
48	1.528	v	a	116	0.984	m	ms
50	1.497	w	v	122	0.959	v	w
52	1.468	w	v	123	0.956	w	a
57	1.404	v	a	125	0.948	v	w
58	1.391	v	a	128	0.937	v	w
59	1.379	s	m	131	0.926	w	ms

N ($= h^2+k^2+l^2$), d Å and I_P taken from Gronvold and Rost (1956) I_G taken from a Gandolfi pattern of Grain 1. Plus 27 more lines to d 0.773 Å

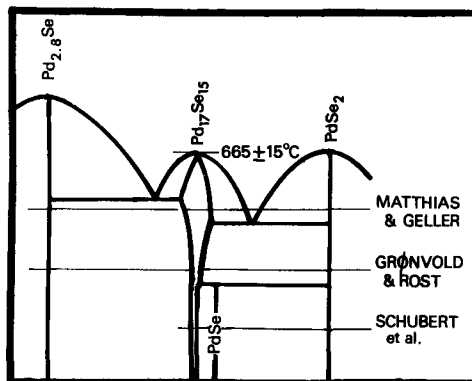


Fig. 3. Sketch of a possible phase diagram for part of the Pd-Se system.

$\text{Pd}_{33.17}\text{Se}_{30.0}$ or $2[\text{Pd}_{17}\text{Se}_{15}]$, confirmed by Geller (1962) from the crystal structure. Matthias and Geller (1958), working with chilled melts of composition Pd₁₇Se found that only the cubic pattern was obtained for x = 1.0, 1.1, or 1.2; like Gronvold and Rost they found that for x = 1.3 or more, the powder pattern showed traces of Pd_{2.8}Se. Schubert et al. (1957) gave cell dimensions for PdSe with the NiAs-type structure, finding it in equilibrium with Pd₁₇Se₁₅ on one side and with PdSe₂ on the other. These observations can be reconciled by a phase diagram such as that sketched in fig 3.

The unit-cell dimensions listed in Table IV show that for Pd₁₇Se₁₅ three determinations in two different laboratories agree to within 0.002 Å, well within the experimental errors. However the fourth result (by Schubert et al., 1957) is significantly larger than the other three and agrees well with our results. We have indexed and extrapolated Gronvold and Rost's data independently and have checked the factor used to convert kX to Å; all figures in Table IV are accurate as claimed and the discrepancy must be explained by assuming Pd₁₇Se₁₅ is a non-stoichiometric compound exhibiting a small range of compositions.

BIBLIOGRAPHY AND REFERENCES

- 1818a Berzelius (J.J.). *Ath. Fys. Kemi, Mineral.* 2, 42-744.
In Swedish; transl. in: *Ann. Chim. Phys.*, 1818, 2, 760-180, 225-267, 337-365; *J. Chem. Phys. (Schweigger)*, 1818, 23, 309-344, 430-484; *Ann. Philos.* 1819, (1), 13, 401-412; (1), 14, 97-106, 257-265, 420-427; (1), 12, 16-27; *Ann. Mines*, 1819, (1), 4, 301-316.
- 1818b Berzelius (J.J.). *Acad. Handl. Stockholm*, 33, 13-22.
- 1829 Zincken (C.). *Ann. Phys. Chem. (Foggedorff)*, 16, 471-498.
- 1876 Rösler (H.). *Ann. Chem. (Liebig)*, 180, 240-245.
- 1895 Rössler (F.). *Z. anorg. Chem.*, 2, 31-77.
- 1925 Moser (L.) and Atynsky (K.). *Monatsh. Chem.*, 54, 235-250.
- 1929 Thomassen (L.). *Z. phys. Chem.*, 2, B, 349-379.
- 1930 Mellor (J.W.), *A Comprehensive Treatise on Inorganic and Theoretical Chemistry*, (Longmans, London) 10, 801, 808.
- 1933 Wohler (L.), Ewald (K.) and Krall (H.G.), *Ber. dtsch. chem. Ges.*, 66, B, 1638-1652.
- 1938 *Gmelin Handbuch der Anorganischen Chemie*, (Verlag Chemie G.m.b.H., Berlin), 8 Auflage, System Nummer 65, Palladium, 296-297.
- 1956 Gronvold (F.) and Rost (E.). *Acta Chem. Scand.*, 10, 1620-1634.
- 1957 _____, *Acta Cryst.* 10, 329-331.
- 1957 Schubert (K.), Breiner (H.), Burkhardt (W.), Gunzel (E.), Haufler (R.), Lukas (H.L.), Vetter (H.), Weget (J.), and Wilkens (M.), *Naturwiss.*, 44, 229-230.
- 1957 Anderko (K.), ed. *The Constitution of Binary Alloys*. (2nd edition of M. Hansen's *Der Aufbau der Zweistofflegierungen*). (McGraw-Hill, New York, 1958), 1125.
- 1958 Matthias (B.T.) and Geller (S.). *J. Phys. Chem. Solids*, 4, 318-319.
- 1958 Ignat'ev (E.S.) and Plaskin (I.N.). *Izv. Vysch. Uchebn. Zaved. Tsvetn. Met.*, (1), 90-94. In Russian; cf. *Chem. Abstr.* 1959, 53, 8986b.
- 1960 Filippov (A.A.) and Smirnov (V.I.). *ibid.*, 2, (6), 55-64. In Russian; cf. *Chem. Abstr.* 1961, 52, 1822d.
- 1960 Kjekshus (A.). *Acta Chem. Scand.*, 14, 1623-1626.
- 1961 Taimi (I.K.) and Rakshpal (R.). *Anal. Chim. Acta*, 25, 438-447.
- 1961 Kulifay (S.M.). *J. Am. Chem. Soc.*, 83, 4916-4919; cf. U.S. Patent 3026175, 1962; cf. *Chem. Abstr.* 1962, 52, P627e.
- 1961 Elliott (R.P.), ed. *First Supplement to K. Anderko's The Constitution of Binary Alloys*, (McGraw-Hill, New York, (1965), 731.
- 1962 Gronvold (F.) and Rost (E.). *Acta Cryst.* 12, 711-713.
- 1962 Geller (S.). *Acta Cryst.* 12, 713-721.
- 1964 Buketov (E.A.), Ugorets (M.Z.) and Pashinakin (A.S.), *Zh. Neorg. Khim.*, 2, (3), 526-529. In Russian; translation in *Russ. J. Inorg. Chem.*, 1964, 2, 292-294.
- 1964 Shunk (F.A.), ed. *Second Supplement to K. Anderko's The Constitution of Binary Alloys* (McGraw-Hill, New York, 1969), 609.
- 1964 Dolivo-Dobrovolskii (V.V.), *Khim. Anal. Tsvetn. Redikh Metal.*, *Akad. Nauk SSSR, Sibirek. Otd., Khim.-Met. Inst.*, 144-155. In Russian; cf. *Chem. Abstr.* 1965, 62, 2668f.
- 1964 Wright (W.D.). *The Measurement of Colour*. 3rd ed. (Halger and Watts Ltd., London).
- 1965 Greivor (T.N.). *Tsvetn. Metal.*, 38, (1), 28-33. In Russian; English translation in *Soviet Metals* (New York), 1965, 27-32.
- 1965 Raub (G.J.), Compton (V.B.), Geballe (T.H.), Matthias (B.T.), Maita (J.P.), and Hull (G.W.Jr.). *J. Phys. Chem. Solids*, 26, 2051-2057.
- 1969 Gronvold (F.), Westrum (E.E.), and Radebaugh (R.). *J. Chem. Eng. Data*, 14, (2), 205-207.
- 1969 Mason (P.K.), Frost (M.T.), and Reed (S.J.B.). *Nat. Phys. Lab. I.M.S. Rep.* 1.
- 1970 Johan (Z.), Picot (P.), Pierrot (R.) and Verbeek (T.). *Bull. Soc. fr. Mineral. Cristallogr.* 93, 476-481.
- 1973 Donnay (J.D.R.) and Ondik (H.). *Crystal Data: Determinative Tables*, 2, Inorganic Cpd., (3rd ed. J.C.P.D.S., U.S.A.), p.C. 310.
- 1974 Clark (A.M.), Criddle (A.J.), and Fejer (E.E.). *Mineral. Mag.* 22, 528-543.
- 1975 Bowie (S.H.U.), Simpson (F.R.) and Atkin (D.). *Fortachr. Mineral.*, 52, Spec. Issue: IMA - Papers 9th Meeting, Berlin - Regensburg, 1974, 567-582.

M 14 | A. Blasi: T-site occupancies in alkali feldspars

CALCULATION OF T-SITE OCCUPANCIES IN ALKALI FELDSPAR FROM REFINED LATTICE CONSTANTS.

Achille Blasi

Istituto di Mineralogia, Petrografia e Geochimica
Università degli Studi
Via Botticell, 23 20133-Milano

Summary. In order to estimate the T-site occupancies in alkali feldspar from refined lattice constants, the involved method developed by Luth (1974) for calculating the structural indicators $\Delta(ba)$ (Stewart and Ribbe, 1969; Stewart and Wright, 1974; Stewart, 1975), $\Delta(b^*o^*)$ (Smith, 1969; 1971), and $\Delta(o^*y^*)$ (Smith, 1969; 1974; Stewart and Ribbe, 1969; Stewart and Wright, 1974; Stewart, 1975) from b , a , b^* and o^* , o^* and y^* , respectively, is reviewed. It is shown that this method furnishes approximate values, which become less accurate the closer the values of the indicators concerned are to the central region of their range. The inaccuracies introduced by using this method can be several tens of times higher than the approximations with which the results are commonly written in the literature.

As an alternative a new method of calculation is proposed which corresponds to a rigorous treatment. It can also be applied for calculating Smith's (1974) indicator $Or(b^*o^*)$, involved in cell dimensions of perthites and anomalous specimens, from refined lattice constants b^* and o^* . The calculation procedure for estimating the appropriate error terms of all these indicators is also given. As all these calculations are tedious and as these quantities are increasingly being used in common mineralogical and petrological practice a computer program available in Fortran IV has been prepared.

In alkali feldspar the indicators of structural state $\Delta(ba)$ (Stewart and Ribbe, 1969; Stewart and Wright, 1974; Stewart, 1975) and $\Delta(o^*y^*)$ (Smith, 1969; 1974; Stewart and Ribbe, 1969; Stewart and Wright, 1974; Stewart, 1975) permit an estimate to be made of Si,Al distribution among the T-sites as well as a distinction between one- and two-step ordering sequences. In all circumstances in which it is convenient, indicator $\Delta(ba)$ can be substituted by indicator $\Delta(b^*o^*)$ (Smith, 1968; 1974).

The value of $\Delta(ba)$ (or $\Delta(b^*o^*)$) can be derived graphically for a given alkali feldspar from its position on the diagram ba vs. o^* (or b^* vs. o^*) with respect to the representative points of the end-members high-calcic-andesine (HS), low-microcline (LM), low-albite (LA), high-albite (HA), which form an irregular quadrilateral (†). In a similar manner the value of $\Delta(o^*y^*)$

(†) For alkali feldspar end-member nomenclature see Smith (1974) and Ribbe (1975).

can be obtained graphically from the diagram o^*y^* vs. y^* with reference to the irregular quadrilateral having as vertices the same end-members used for the ba plot, except HS, which is substituted by the end-member MF (monoclinic feldspar).

Luth (1974) has pointed out the disadvantages of this procedure and consequently has proposed an analytical method of calculation.

Since this method appeared approximate when first examined, the present study was undertaken in order to determine more precisely the limitations of Luth's (1974) method and to devise a new calculation procedure corresponding to a rigorous treatment, which can also be applied for calculating Smith's (1974) indicator $Or(b^*o^*)$ from refined lattice constants b^* and o^* . In addition, it was thought appropriate to provide a calculation procedure for estimating the error terms of all these indicators.

Basic Features. According to the well-known assumptions that form the basis for the Ribbe-Stewart-Wright interpretation of variation in unit cell parameters of alkali feldspar with Si,Al ordering, there is a continuous and uniform variation of $\Delta(ba)$ values in the range between 0.5 and 1 (†) along

(†) Smith (1974) normalizes the indicator $\Delta(b^*o^*)$ between 0 and 1.

the sides HS-LM and HA-LA of the quadrilateral HS-LM-LA-HA on the ba plot, while there is a continuous and uniform variation of $\Delta(o^*y^*)$ values included between 0 and 1 on the o^*y^* plot along the sides MF-LM and HA-LA of the quadrilateral MF-LM-LA-HA. In both cases, the quadrilaterals can be contoured linearly by iso- $\Delta(ba)$ and iso- $\Delta(o^*y^*)$ straight lines respectively.

The indicators of structural state $\Delta(ba)$ (or $\Delta(b^*o^*)$) and $\Delta(o^*y^*)$ estimate sum and difference, respectively, for Al content of T-sites T_{10} and T_{1m} . Consequently, as $T_{10}+T_{1m}+T_{20}+T_{2m}=1$, it is possible to obtain the values of T_{10} , T_{1m} , T_{20} and T_{2m} which, according to Kroll's (1971) notation, represent the probability of finding Al in the T_{10} , T_{1m} , T_{20} , T_{2m} sites respectively.

Some caveats have been made regarding use of this procedure, particularly by Luth (1974), Smith (1974), and Stewart and Wright (1974); but Stewart (1975) points out that, for practical purposes, this interpretation of the available data is adequate for every geological problem and natural specimen and also for almost all known sophisticated mineralogical problems.

Smith (1974) has pointed out that one can also derive indicator $Or(b^*o^*)$ from the quadrilateral HS-LM-LA-HA plotted on the b^*o^* plot. Smith (1974) fixes a continuous and uniform conventional variation of $Or(b^*o^*)$ values ranging from 0 to 1 along the sides HA-HS and LA-LM, and further contours the quadrilateral linearly by iso- $Or(b^*o^*)$ straight lines. The indicator $Or(b^*o^*)$ can be used in a diagram versus o^* , which is involved in cell dimensions of perthites and anomalous specimens.

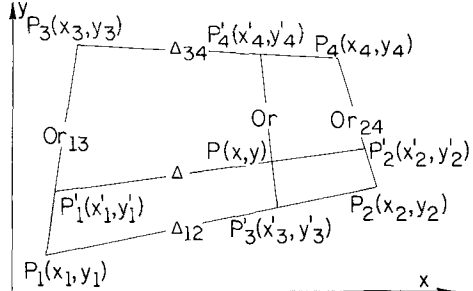


Fig. 1. Plot of xy of the reference quadrilateral in recommended orientation used to obtain equations to calculate $\Delta(ba)$, $\Delta(b^*o^*)$, $\Delta(o^*y^*)$ and $Or(b^*o^*)$ in alkali feldspar.

For the sake of conciseness and in order to carry out a general treatment, let us consider, instead of the rectangular systems ba (or b^*o^*) and o^*y^* , a single rectangular system of axes x along which the coordinate values increase from the origin toward the right and upward (Fig. 1).

The end-members HS (or MF), LA, LM are labeled with the notations P_1 , P_2 , P_3 , P_4 , respectively; a generic value of the indicators $\Delta(ba)$ (or $\Delta(b^*o^*)$) and $\Delta(o^*y^*)$ is indicated by the notation Δ ; the extreme values of these indicators are labeled with the notations Δ_{12} and Δ_{34} . In a similar manner, a generic value of $Or(b^*o^*)$ is indicated by the symbol Or , while its extreme values are labeled with Or_{13} and Or_{24} .

In the quadrilateral $P_1P_2P_3P_4$ the locus of points of equal Δ (or Or) is represented, for each given value of Δ (or Or), by a straight line which intersects sides P_1P_2 and P_3P_4 (or P_2P_3 and P_4P_1) at the two points characterized by that given value of Δ (or Or).

If the values of Δ_{12} and Δ_{34} (or Or_{13} and Or_{24}) and those of the quadrilateral vertex coordinates are known, it is possible to calculate the corresponding value of Δ (or Or) for each point $P(x, y)$ of the quadrilateral, assuming coordinates x and y are known.

The reference values of the vertex coordinates of the quadrilaterals, involved in the calculations, have been chosen taking account of the unit cell dimensions of the extreme end-members of synthetic and natural alkali feldspars and also of their experimental uncertainties. Gubser and Leves (1967), Stewart and Ribbe (1969), and Luth (1974) have proposed reference values for these vertices but only with respect to some unit cell parameters; Smith (1974), and Stewart and Wright (1974) have proposed more up-to-date reference values for all unit cell dimensions both direct and reciprocal.

Smith (1974) has pointed out the disadvantages of this procedure and consequently has proposed an analytical method of calculation.

Since this method appeared approximate when first examined, the present study was undertaken in order to determine more precisely the limitations of Luth's (1974) method and to devise a new calculation procedure corresponding to a rigorous treatment, which can also be applied for calculating Smith's (1974) indicator $Or(b^*o^*)$ from refined lattice constants b^* and o^* . In addition, it was thought appropriate to provide a calculation procedure for estimating the error terms of all these indicators.

$$(\lambda - \Delta \lambda') \Delta + (\mu - \Delta \mu') y + (\nu - \Delta \nu') = 0.$$

Each straight line is characterized by one value of Δ . The corresponding value of Δ at each point $P(x, y)$ can be determined if the coefficients λ' , μ' , ν' , λ , μ , ν are known. However one can determine only four of these coefficients in view of the number of vertices of quadrilateral $P_1P_2P_3P_4$; two coefficients are thus arbitrary. If one lets one of these be equal to zero and the other equal to 1, one arrives at a form that enables the expressions given by Luth to be obtained. In particular they are derived by letting $\mu=0$ and $\nu=1$. In this hypothesis one obtains the relationship:

$$\Delta = (\nu' + \lambda' x + \nu) / (\nu + \lambda' x)$$

which reproduces the form of Luth's equations. It should be borne in mind that in (1) one must replace x by b , b^* , or y and y by o^* , o^* , or o^* . The coefficients of (1) are obtained by solving the following four simultaneous equations:

$$\Delta_{12} \nu' + \lambda_{12}' x_1 - \nu = \lambda_{12}' x_2 - \nu = 0; \quad \Delta_{12} \nu' + \lambda_{12}' x_2 - \nu - \lambda_{34}' x_2 + \nu = 0; \quad (2)$$

$$\Delta_{34} \nu' + \lambda_{34}' x_3 - \nu = \lambda_{34}' x_4 - \nu = 0; \quad \Delta_{34} \nu' + \lambda_{34}' x_4 - \nu - \lambda_{12}' x_4 + \nu = 0.$$

For this purpose a Fortran IV program has been prepared, which also permits the structural indicator Or to be computed. Or , by placing in (2) the values of the direct or reciprocal lattice constants for alkali feldspar end-members used by Luth, it has been possible to obtain values of the coefficients λ' , μ' , ν' , λ , μ , ν , identical to those appearing in the various formulae calculated by Luth.

By using the vertex coordinates proposed by Smith (1974) for the quadrilaterals $P_1P_2P_3P_4$ the writer has also calculated the following other relationships:

$$\Delta(ba) = (-0.66437 - 0.494547ba) / (1.94200 - 0.138549b) \quad (3)$$

$$\Delta(b^*o^*) = (0.008738 - 2.16049b^*o^*) / (0.003466 - 0.09733b^*) \quad (4)$$

$$\Delta(o^*y^*) = (88.683 - 1.98377y^*) / (-22.5530 + 1.9942y^*) \quad (5)$$

Limits of $\Delta(b^*o^*)$ ranging between 0.5 and 1 have been used to calculate equation (5).

Rigorous treatment.

Calculation of Δ . In order to calculate the values of the indicators Δ it is necessary to know and solve with respect to Δ the equation of the iso- Δ straight line on which the point $P(x, y)$ lies in the irregular quadrilateral $P_1P_2P_3P_4$ (Fig. 1). The straight line $(x - x_1) / (x_2 - x_1) = (y - y_1) / (y_2 - y_1)$ intersects sides P_1P_2 and P_3P_4 respectively at the points $P_1'(x_1', y_1')$ and $P_2'(x_2', y_2')$, and if the coordinates of the points P_1' and P_2' are expressed as functions of Δ , Δ_{12} , Δ_{34} and of the quadrilateral vertex coordinates we can deduce the quadratic form:

$$A\Delta^2 + B\Delta + C = 0 \quad (6)$$

where: $A = (x_4 - x_2)(y_3 - y_1) - (x_3 - x_1)(y_4 - y_2)$, $B = (\Delta_{34} - \Delta_{12}) \{ (x_1 - x_2)(y_3 - y_1) - (x_2 - x_1)(y_4 - y_2) \} + (\Delta_{34} - \Delta_{12}) \{ (x_1 - x_2)(y_3 - y_1) - (x_3 - x_1)(y_4 - y_2) \} + 2\Delta_{12} \Delta_{34} (x_2 - x_1)(y_3 - y_1) - 2\Delta_{12} \Delta_{34} (x_3 - x_1)(y_4 - y_2)$, $C = \Delta_{12}^2 \{ (x_2 - y_1) - y_1(x_2 - x_1) \} + \Delta_{34}^2 \{ (x_4 - y_2) - y_2(x_4 - x_3) \} + (x_1 - x_2)(y_3 - y_1) - (x_3 - x_1)(y_4 - y_2) + \Delta_{12} \Delta_{34} \{ (x_1 - y_3) + (y_3 - y_1) \} - y_1(x_4 - x_3) + (x_2 - x_1) + (x_1 - x_2)(y_3 - y_1) - (x_3 - x_1)(y_4 - y_2)$.

From an examination of the coefficients of equation (6) it will be seen that, in particular, the condition $A=0$ expresses the parallelism of the straight lines passing through the points P_1P_2 and P_3P_4 respectively. If this condition were satisfied equation (6) would reduce to the first degree. As, in fact, $A \neq 0$, $\Delta = (-B \pm (B^2 - 4AC)^{1/2}) / 2A$, which in practice gives two real and unequal solutions one of which is included in the range between Δ_{12} and Δ_{34} , and of course is the solution to accept. With the orientation of the rectangular system xy as previously defined, it has been verified that, of the real and unequal solutions furnished by (6) the solutions of $\Delta(ba)$ and $\Delta(o^*y^*)$ to accept are those obtained from the positive square root, whereas to arrive at $\Delta(b^*o^*)$ the negative of the square root has to be used.

Calculation of Or . In addition to a straight line iso- Δ , a straight line iso- Or also passes through each point $P(x, y)$ of the quadrilateral $P_1P_2P_3P_4$ (Fig. 1). The equation of the straight line iso- Or that passes through $P(x, y)$ and intersects sides P_1P_2 and P_3P_4 at the points $P_1''(x_1'', y_1'')$ and $P_2''(x_2'', y_2'')$ respectively is $(x - x_1'') / (x_2'' - x_1'') = (y - y_1'') / (y_2'' - y_1'')$.

By expressing the coordinates of the points P_1'' and P_2'' as functions of Or , Or_{13} , Or_{24} , and of the coordinates of the quadrilateral vertices, we arrive at a quadratic form with respect to Or :

Table I. $\Delta(ba)$ values of hypothetical alkali feldspars.

Field I (+)			Field II (+)			Field III (+)		
$b(\text{\AA})$	$a(\text{\AA})$	$\Delta(ba)$	$b(\text{\AA})$	$a(\text{\AA})$	$\Delta(ba)$	$b(\text{\AA})$	$a(\text{\AA})$	$\Delta(ba)$
(1)	(2)	(3)	(4)	(5)	(6)	(7)	(8)	(9)
12.7861	1.000	1.000	12.8749	1.1900	1.000	12.9631	1.2214	1.000
12.7960	1.1540	0.953	12.8830	1.1855	0.953	12.9667	1.2158	0.953
12.8042	1.1490	0.906	12.8944	1.1822	0.906	12.9742	1.2116	0.906
12.8165	1.1455	0.858	12.8992	1.1765	0.858	12.9830	1.2079	0.858
12.8223	1.1396	0.809	12.9033	1.1705	0.809	12.9870	1.2024	0.809
12.8308	1.1347	0.759	12.9110	1.1658	0.759	12.9921	1.1973	0.759
12.8411	1.1305	0.709	12.9231	1.1609	0.709	13.0056	1.1943	0.709
12.8481	1.1250	0.658	12.9255	1.1563	0.658	13.0062	1.1886	0.658
12.8610	1.1219	0.606	12.9357	1.1525	0.606	13.0143	1.1847	0.606
12.8649	1.1151	0.554	12.9464	1.1491	0.554	13.0213	1.1787	0.554
12.8765	1.1115	0.500	12.9520	1.1436	0.500	13.0263	1.1752	0.500

(+) With reference to the quadrilateral HS-LM-LA-HA (see text).
 (*) Calculated from equation (6).
 (‡) Calculated from equation (3).

Table II. $\Delta(a^{**})$ values of hypothetical alkali feldspars.

Field I (+)			Field II (+)			Field III (+)			
$a^{**}(\%)$	$\gamma^{**}(\%)$	$\Delta(a^{**})$	$a^{**}(\%)$	$\gamma^{**}(\%)$	$\Delta(a^{**})$	$a^{**}(\%)$	$\gamma^{**}(\%)$	$\Delta(a^{**})$	
(1)	(2)	(3)	(4)	(5)	(6)	(7)	(8)	(9)	
86.443	90.480	1.000	1.000	88.364	91.359	1.000	1.000	90.339	92.263
86.435	90.247	0.900	0.890	88.438	91.173	0.900	0.890	90.296	92.032
86.353	89.980	0.800	0.783	88.240	90.861	0.800	0.783	90.250	91.800
86.320	89.736	0.700	0.678	88.356	90.696	0.700	0.678	90.230	91.580
86.260	89.479	0.600	0.575	88.159	90.383	0.600	0.575	90.220	91.365
86.234	89.248	0.500	0.474	88.234	90.200	0.500	0.474	90.145	91.119
86.213	89.000	0.400	0.375	88.079	89.906	0.400	0.375	90.098	90.866
86.161	88.747	0.300	0.278	88.159	89.726	0.300	0.278	90.079	90.667
86.081	88.480	0.200	0.184	87.951	89.480	0.200	0.184	90.003	90.420
86.081	88.253	0.100	0.091	88.059	89.240	0.100	0.091	89.982	90.200
86.029	88.000	0.000	0.000	87.900	88.942	0.000	0.000	89.921	89.960

(+) With reference to the quadrilateral MF-LM-LA-HA (see text).
 (*) Calculated from equation (6).
 (‡) Calculated from equation (3).

$$D0a^2 + E0a + F = 0 \quad (7)$$

where: $D = (a_1 - a_2)(a_2 - a_3)(a_3 - a_1)$
 $E = (Or_2 - Or_1)(a_1 + a_2) + (Or_3 - Or_2)(a_2 + a_3) + (Or_1 - Or_3)(a_3 + a_1) + (Or_2 + Or_3)(a_1 + a_2) + (Or_1 + Or_3)(a_2 + a_3) + (Or_2 + Or_1)(a_3 + a_1) - 2Or_1Or_2 - 2Or_2Or_3 - 2Or_3Or_1$
 $F = Or_1^2(a_1 + a_2 + a_3) + Or_2^2(a_2 + a_3 + a_1) + Or_3^2(a_3 + a_1 + a_2) - Or_1Or_2(a_1 + a_2) - Or_2Or_3(a_2 + a_3) - Or_3Or_1(a_3 + a_1) - Or_1Or_2Or_3(a_1 + a_2 + a_3)$

As in practice $D \neq 0$ (i.e., the quadrilaterals side P_1P_2 and P_2P_3 are not parallel), $Or = (E \pm \sqrt{E^2 - 4DF})/2D$, which gives two real and unequal solutions, one of which falls in the interval between Or_1 and Or_2 , and of course is the solution to (7).
 With the orientation of the quadrilateral $P_1P_2P_3P_4$ as previously defined, it has been noted in particular that, of the two real and unequal solutions, the value of $Or(ba^{**})$ to accept is that obtained with the positive square root of the discriminant.

Conclusions.

Using the reference values proposed by Smith (1974) for alkali feldspar end-members, the differences between the results obtained by means of Luth's (1974) equations and those derived from the rigorous treatment provided in the present paper are summarized in Tables I and II. Table I gives a set of values of $\Delta(ba)$ calculated by means of equations (3) and (6) for three different fields of the quadrilateral HS-LM-LA-HA. Field I is located about the quadrilateral side HS-LA, field II about the straight line intersecting the middle of the sides HA-HS and LA-LM, field III about the side HS-LM. Table II shows a set of values of $\Delta(a^{**})$ calculated by means of equations (5) and (6) for the three analogous fields of quadrilateral MF-LM-LA-HA.

Comparison of the results furnished by the two procedures shows that: the values obtained with (3) and (6) and those obtained with (5) only coincide at each extreme of $\Delta(ba)$ and $\Delta(a^{**})$; the greatest differences found among the values obtained are, in $\Delta(ba) \approx 0.75$ and in $\Delta(a^{**}) \approx 0.50$; these differences gradually diminish as the extremes of a are approached; they are in all cases greater in the values of $\Delta(a^{**})$ than in the values of $\Delta(ba)$; and for a given $\Delta(ba)$ the differences between the values obtained from (3) and (6) decrease slightly in a systematic way from field I to field III.

As the values of $\Delta(ba)$ and $\Delta(a^{**})$ determined with Luth's formulæ are greater and smaller respectively than those calculated by means of (6), subdivision of the quadrilaterals HS-LM-LA-HA and MF-LM-LA-HA by means of iso- Δ straight lines calculated from (3) and (6) and from (8) gives rise to the sections displayed in Figs. 2 and 3.

In conclusion, the equations devised by Luth (1974) for calculating the structural indicators $\Delta(ba)$, $\Delta(ba^{**})$, $\Delta(a^{**})$ of alkali feldspar furnish values that become farther from the true ones the closer the values of these indicators are to the central region of their range.

As results are commonly rounded off until they contain three (cf. Crosby, 1971; Guidotti, Hrad, and Tuttle, 1973; Martin, 1974; Stewart and Wright, 1974; Steiner, 1975; Debye, 1975; Bess and Vitale, 1976) or four decimal places (cf. Luth, Martin, and Fenn, 1974), it also seems

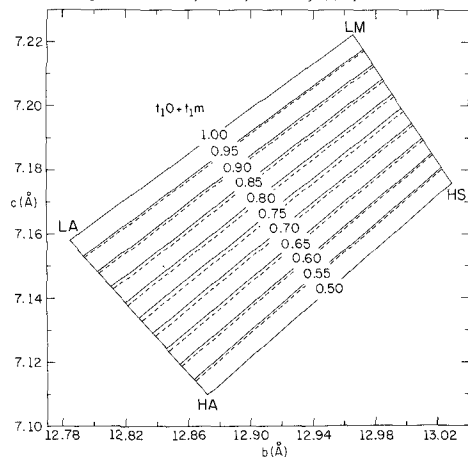


Fig. 2. Plot of ba of alkali feldspar using end-member coordinates for high-salidine (HS), low-microcline (LM), low-albite (LA), and high-albite (HA) as given by Smith (1974). The quadrilateral, contoured for $t_0 - t_1m$, shows the differences between the straight lines representing the $\Delta(ba)$ values calculated from equation (6) (solid lines) and those obtainable from equation (3) (dashed lines).

worthwhile pointing out that the inaccuracies introduced by using Luth's equations can be several tens of times higher than the approximations with which the results are usually written.

The formulæ devised in the present investigation for calculating both structural indicators $\Delta(ba)$, $\Delta(ba^{**})$, $\Delta(a^{**})$ and Smith's (1974) indicator $Or(ba^{**})$ entail tedious computations. As these quantities are being increasingly used in common mineralogical and petrological practice, a computer program available in Fortran IV has also been prepared, which permits these indicators and their respective variances to be calculated. The calculation procedure for the variances is given in the attached Appendix.

Appendix.

Estimate of error terms. The error terms in $\Delta(ba)$, $\Delta(ba^{**})$, $\Delta(a^{**})$ and $Or(ba^{**})$ can be estimated by a graphical method. Geometrically the point $P(x, y)$, the Δ (or Or) value and the error in Δ (or Or) of which it is desired to know, is at a center of a rectangle whose sides are $2\sigma(x)$ and $2\sigma(y)$ respectively. Among the iso- Δ (or iso- Or) straight lines passing through the four vertices, two touch the rectangle without intersecting it; they are the furthest from the iso- Δ (or iso- Or) straight line passing through the center and furnish two differences with respect to the Δ (or Or) value of this last line. The highest of these differences represents the error term in Δ (or Or) determined graphically (these two differences are nearly equal in practice).

The values of the errors determined graphically, in the particular quadrilaterals considered, coincide in practice with those derived from the equation:

$$\sigma(\Delta, Or) = |[\sigma(\Delta, Or)/\sigma x] \sigma(x) + [\sigma(\Delta, Or)/\sigma y] \sigma(y)| \quad (8)$$

which represents, apart from the absolute value symbol, the total differential of Δ (or Or) and furnishes the maximum error in the absence of any correlation among the errors.

As the quadrilaterals involved are irregular, estimating error terms by a graphical method is very time-consuming and furthermore furnishes values which, as we have seen, can be too high.

For these reasons, it is better to calculate these error terms by means of the Law of Propagation of Errors, according to which, in general, the variance $\sigma^2(f)$ of a function f of p parameters ξ_p , i.e. $f(\xi) = f(\xi_1, \xi_2, \dots, \xi_p)$, is given by the expression:

$$\sigma^2(f) = \sum_{i=1}^p \left(\frac{\partial f(\xi)}{\partial \xi_i} \right)^2 \sigma_{\xi_i}^2 \quad (9)$$

where V_{ij} is the variance-covariance matrix of the parameters ξ_p , and $\xi = \xi_1, \xi_2, \dots, \xi_p$ represent the true values of $\xi = \xi_1, \xi_2, \dots, \xi_p$. In practice, estimates of these quantities would usually have to be used and one should always ensure that the quantities $(\xi_p - \xi_p)$ are small enough to justify truncation of the Taylor expansion of $f(\xi)$ about the point $\xi = \xi$ at the first order in $(\xi_p - \xi_p)$ (Martin, 1971).
 Error terms $\sigma \Delta$. On applying (9), error in Δ can be evaluated from the following formula:

$$\sigma_{\Delta}^2(\Delta) = (\sigma a / \sigma x)^2 V_{mm} + (\sigma a / \sigma y)^2 V_{nn} + 2(\sigma a / \sigma x)(\sigma a / \sigma y) V_{mn} \quad (10)$$

where V_{mm} and V_{nn} represent the variances and V_{mn} the covariances as ob-

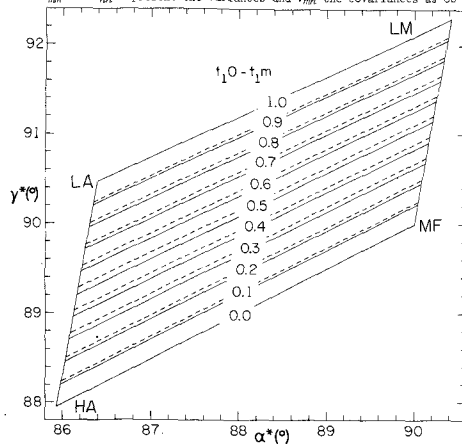


Fig. 3. Plot of a^{**} of alkali feldspar using the reference points for monoclinic feldspar (MF), low-microcline (LM), low-albite (LA), and high-albite (HA) as given by Smith (1974). The quadrilateral, contoured for $t_0 - t_1m$, shows the differences between the straight lines of the $\Delta(a^{**})$ values calculable from equation (6) (solid lines) and those obtainable from equation (3) (dashed lines).

obtained from reciprocal or direct lattice constant variance-covariance matrices. The subscripts m and n assume values 2, 3 or 4 and 6 according to whether delta is a function of the edges or of the unit cell angles. Furthermore:

delta/2a = (1/2A) (delta/2a) + 1/4 (delta^2/4AC) [(E/2A) (delta/2a) - (delta/2a)] (11)

delta/2b = (delta/2a) (delta/2a) / (y4-y3-y2-y1)

delta/2c = delta/2a (y2-y1) + delta/2c (y4-y3) - delta/2c delta/2a (y4-y3-y2-y1)

delta/2d = (1/2A) (delta/2a) + 1/4 (delta^2/4AC) [(E/2A) (delta/2a) - (delta/2a)] (12)

delta/2e = (delta/2a) (delta/2a) / (x1-x2-x3-x4)

delta/2f = delta/2a (x2-x1) - delta/2a (x1-x2) + delta/2a delta/2a (x1-x2-x3-x4)

Equations (11) and (12) must be used with the positive sign or the negative sign according to whether the value of delta accepted has been obtained from (6) with the positive or negative square root of the discriminant.

Variance and covariance terms required to solve equation (10) are usually available on the output of the lattice constant refinement programs. Incidentally, for correct utilization of (10) it should be borne in mind that, as far as unit cell angles are concerned, computer programs usually furnish variance and covariance values in rad^2 and standard deviation values, i.e. the square root of the variances, in degree.

If on applying (8) one assumes that the errors are uncorrelated, i.e. cov(Vm, Vn) = 0, then

sigma^2(Vm) = sigma^2(Vm) + sigma^2(Vn) + sigma^2(Vm) (delta/2a) + sigma^2(Vm) (delta/2a)^2 (13)

The values of the standard deviation given by (10) are generally slightly greater than those furnished by (13), but in both cases are smaller than those obtained graphically.

Error norms in phi. The standard deviation sigma(phi) of phi(phi) can be calculated in a similar way to that of delta by means of the law of Propagation of Errors:

sigma^2(phi) = (delta/2a)^2 sigma^2(Vm) + (delta/2a)^2 sigma^2(Vn) + (delta/2a)^2 sigma^2(Vm) (delta/2a) (14)

where Vm, Vn, Vm, Vm have been previously defined. In this case, the subscripts m and n of course assume values 2, 3 or 4 in the reciprocal lattice constant variance-covariance matrix. Moreover:

delta/2a = (1/2A) (delta/2a) + 1/4 (delta^2/4AC) [(E/2A) (delta/2a) - (delta/2a)] (15)

delta/2b = (delta/2a) (delta/2a) / (y4-y3-y2-y1)

delta/2c = delta/2a (y2-y1) + delta/2c (y4-y3) - delta/2c delta/2a (y4-y3-y2-y1)

delta/2d = (1/2A) (delta/2a) + 1/4 (delta^2/4AC) [(E/2A) (delta/2a) - (delta/2a)] (16)

delta/2e = (delta/2a) (delta/2a) / (x1-x2-x3-x4)

delta/2f = delta/2a (x2-x1) - delta/2a (x1-x2) + delta/2a delta/2a (x1-x2-x3-x4)

When applying (14), it should be noted that double signs must be used in expressions (15) and (16) in a similar way to those used in calculating the errors in delta. If one assumes that the errors are uncorrelated the cross product of equation (14) becomes zero.

Acknowledgments. I wish to thank Prof. Joseph V. Smith for his encouragement and advice, and Prof. Giuseppe Schiavato for valuable suggestions.

Financial support was provided by C.N.R. (Italian National Research Council). All computations were carried out on an Univac 1106 computer at the Milan University Computer Center.

References.

Bau (A.) and Vitaliano (C.F.), 1975. Sanidine from the Mesa Falls Tuff, Ashton, Idaho. Am. Mineral. 60, 405-50.
Crosby (P.), 1971. Composition and structural state of alkali feldspars from charnockitic rocks on Whiteface Mountain, New York. Am. Mineral. 56, 1768-811.
Dellove (F.), 1975. Excess Gibbs energy of microcline-low albite alkali feldspars at 800°C and 1 bar, based on fused alkali bromide ion-exchange experiments. Am. Mineral. 60, 972-84.
Guidotti (C.V.), Herd (H.K.), and Tuttle (C.L.), 1973. Composition and structural state of K-feldspars from K-feldspar + sillimanite grade rocks in northwestern Maine. Am. Mineral. 58, 105-16.
Gusev (R.) and Laves (F.), 1967. On X-ray properties of "adularia", (K,Na)AlSi3O8. Schweiz. Mineral. Petrogr. Mitt. 47, 177-88.
Kroll (H.), 1971. Determination of Al/Si distribution in alkali feldspars from X-ray powder data. Neues Jahrb. Mineral., Monatsch. 91-4.
Luth (W.C.), 1974. Analysis of experimental data on alkali feldspars: unit cell parameters and solvi. In Mackenzie (W.S.) and Zussman (J.), eds. The Feldspars: Proceedings of a NATO Advanced Study Institute (Manchester 11-21 July 1973). (Manchester University Press. Crane, Russak & Company, Inc., New York). 249-265.
Martin (B.R.), and Penn (P.M.), 1974. Peralkaline alkali feldspar solvi. Ibid. 297-312.
Martin (B.R.), 1971. Statistics for Physiocrats. Academic Press (London).
Martin (B.R.), 1974. The alkali feldspar solvi: the case for a first-order break on the X-lim. Bull. Soc. Fr. Mineral. Crist. 97, 346-55.
Smith (J.V.), 1968. Cell dimensions, c/a, c/b, c/g, y of alkali feldspars permit qualitative estimates of Si/Al ordering: albite ordering process (abstr.). Geol. Soc. Am. Abstr. Progr., Mexico City, 283.
— 1974. Feldspar Minerals. Vol. 1. Crystal Structure and Physical Properties. Springer-Verlag (Berlin).
Stewart (D.B.), 1975. Lattice parameters, composition, and Al/Si order in alkali feldspar. In Ribbe (P.H.), ed. Feldspar Mineralogy: Mineralogical Society of America, Short Course Notes. Min. Soc. Am., Washington, D.C., pp. 81-82.
— and Ribbe (P.H.), 1969. Structural explanation for variation in cell parameters of alkali feldspar with Al/Si ordering. Am. J. S. 267A, 444-62.
— and Wright (T.L.), 1974. Al/Si order and symmetry of natural alkali feldspars, and the relationship of strained cell parameters to bulk composition. Bull. Soc. Fr. Mineral. Crist. 97, 356-77.
Ribbe (P.H.), 1975. The chemistry, structure and nomenclature of feldspars. In Ribbe (P.H.), ed. Feldspar Mineralogy: Mineralogical Society of America, Short Course Notes. Min. Soc. Am., Washington, D.C., pp. R1-R52.

J.F.W.Bowles : History of Fe3O4-FeTiO3 grains (App.)

An estimation of the probable errors of the method of tracing the cooling history of complex magnetite-ilmenite grains and a discussion of the results produced by using different methods of treatment of the minor elements contained in these minerals when using the Buddington and Lindsley (1964) geothermometer.

(Appendix to "A method of tracing the temperature and oxygen-fugacity histories of complex magnetite-ilmenite grains", this vol. pp 103-109)

John F W Bowles
Department of Geology, University College London WC1E 6BT
Present address: Institute of Geological Sciences, 64/78 Gray's Inn Road
London WC1X 8NG

Estimation of errors in the method of calculation used by Bowles (1977)

The formation of ilmenite from titanomagnetite frequently shows separate generations of exsolved ilmenite. Bowles (1977) used microprobe analyses of host magnetite and two generations of ilmenite with an estimate of the volume of each phase to derive compositions representing different stages in the cooling history of a complex magnetite ilmenite grain. Use of the Buddington and Lindsley (1964) geothermometer provided two points in the temperature and oxygen-fugacity history of the specimen. In this appendix a comparison of the errors of measurement is used to determine the likely errors in the result, to check the validity of that result.

The quantity of TiO2 in the titanomagnetite is directly related to the quantity of ulvöspinel that is calculated. One standard deviation of the microprobe X-ray counts leads to an estimated error of +/- 0.12% TiO2 on the measured value of 8.07% TiO2. This error encompasses the X-ray statistical variation and the mineralogical variation between 20 measured localities on 5 adjacent magnetites. Only minor amounts of TiO2 are subtracted when the minor elements are expelled to give 23.7 +/- 0.35% ulvöspinel. Since the magnetite-ulvöspinel contours on the Buddington and Lindsley (1964) diagram are the most steeply inclined they have the greatest influence on the horizontal, temperature axis. At the condition of equilibrium of the magnetite with the ilmenite lamellae a variation of 10% ulvöspinel results in a temperature variation of 25°C, hence the calculated error of 0.35% ulvöspinel gives a temperature error of +/- 0.88°C and a value

of +/- 1°C is adopted here.

The quantity of total FeO contained in the ilmenite lamellae is 41.19% with an error of +/- 0.33% estimated from one standard deviation of the 20 microprobe measurements on ilmenite lamellae within the five adjacent magnetite grains. Only a small proportion of the measured Fe forms the 3.02% hematite but since a subtraction is involved the whole of the error has been loaded onto the hematite. The less steeply inclined ilmenite-hematite lines of the Buddington and Lindsley diagram indicate a greater influence on oxygen fugacity and at the lower temperature equilibration 2% hematite represents a change of about 1 log fO2 in oxygen fugacity. Thus an error of 0.33% hematite represents an error of 0.17 log fO2 oxygen fugacity and a value of +/- 0.2 is taken here.

At the condition of equilibrium of the granular ilmenite the influence of errors in the microprobe results for the granular ilmenite is less, since the lines on the Buddington and Lindsley diagram are spaced more closely and reasoning similar to the above leads to -11.5 +/- 0.04 log fO2 for the oxygen fugacity measurement. In the determination of the earlier magnetite composition, errors introduced by other techniques must be considered. The change in cell size of the magnetite with composition is small, so the effect of errors in composition on cell size may be neglected. However the influence of the less precise point counting technique must be considered here. The same five adjacent magnetite grains for which microprobe results were obtained, were covered by point counting on equally spaced linear traverses and 1019 points were counted. The five grains in different orientations show wide variation in the width of the ilmenite lamellae at their intersection with the polished surface. However, since for each grain the relative orientation of the magnetite to the ilmenite is preserved, the measured value of the ratio of area is little affected by changes in orientation. The proportion of ilmenite lamellae determined in this way is 16.1 +/- 2.03% with the error determined at the 95% confidence limit. This figure is used (Bowles, 1977) to determine that the number of atoms of Fe and Ti within the ilmenite is (6.12 +/- 0.76) x 10^21 and (33.60 +/- 0.84) x 10^21 within the magnetite. A total of (39.72 +/- 1.14) x 10^21 atoms, of which (5.61 +/- 0.16) x 10^21 are Ti, are calculated for the magnetite producing a Ti/(Ti + Fe) ratio of 0.141 +/- 0.004 and leading to a molecule containing 42.3 +/- 1.12% ulvöspinel. At the conditions of equilibration of the granular ilmenite a change of 10% ulvöspinel corresponds to a 29°C change in temperature and leads to a temperature of 930 +/- 3.2°C. Because the lines on the Buddington and Lindsley diagram intersect at a low angle, an error on one set of lines influences estimates of error on the other axis